

ACTIVATED CHARCOAL: A NATURAL PROTECTIVE MEASURE AGAINST THE LINGUAL DEGENERATIVE EFFECT OF TACROLIMUS IMMUNOSUPPRESSANT

Hagar Sherif Abdel Fattah^{1,2*} PhD, Marwa M. Essawy^{3,4} PhD, Amira S. Eissa¹ PhD,

ABSTRACT

OBJECTIVE: The presented work was conducted to test the effectiveness of activated charcoal on the lingual mucosa of male rats subjected to the immunosuppressive drug tacrolimus.

DESIGN: After random allocation of thirty healthy male Wistar albino rats into three groups (10 per group), in group 1 {control group} animals received saline, whereas those in group 2 {the tacrolimus (TAC) group} received daily subcutaneous injections of the immunosuppressant for 3 weeks. In the third cohort group 3 {tacrolimus and activated charcoal; TAC+AC}, rats received activated charcoal orally administered beside the TAC for 3 weeks. After three weeks of treatment, the evaluation of dissected tongues exempted histological, immunohistochemical, and morphometrical analyses.

RESULTS: Histological findings revealed mucosal and connective tissue degenerative changes induced by TAC. However, the AC group showed the preserved structure of the lingual mucosa and associated minor salivary glands. The immunohistochemical detection of Melan-A revealed the profound drop in the mean area percent and optical density of melanophages to $0.82 \pm 0.2\%$ and 0.12 ± 0.01 , respectively, upon AC counteraction of TAC melanosis.

CONCLUSIONS: AC exerted protective action against the degenerative effect of TAC on the lingual mucosa, encouraging its adjuvant uptake throughout the immunosuppressants course.

KEYWORDS: Charcoal; Immunosuppressive drugs; Melan-A; Rats; Tacrolimus; Tongue.

1 Department of Oral Biology, Faculty of Dentistry, Alexandria University, Champollion Street, Alexandria 21526, Egypt.

2 Department of Oral Biology, Faculty of Dentistry, Beirut Arab University, Lebanon.

3 Department of Oral Pathology, Faculty of Dentistry, Alexandria University, Champollion Street, Alexandria 21526, Egypt.

4 Center of Excellence for Research in Regenerative Medicine and Applications (CERRMA), Faculty of Medicine, Alexandria University, Alexandria 21526, Egypt.

* Corresponding Author:

Email: Amira.salama@alexu.edu.eg

INTRODUCTION

Immunosuppression following organ transplant is crucial to avoid acute and chronic rejection, minimizing the risks of graft loss and subsequent morbidity. Masking the immune system, immunosuppressive agents include steroids, antiproliferative agents, calcineurin inhibitors, and target rapamycin inhibitors [1,2].

Tacrolimus (TAC), known as FK506 or Fujimycin, is one of the macrolides calcineurin inhibitors and is the backbone of most immunosuppressive regimens discovered in 1984 in Japan. Shortly after its application in clinical practice in 1989, it decreased rejection and enhanced organ function over the long-term post-transplant, after which TAC became the gold standard for solid organ transplantation. Also, autoimmune diseases irresponsive to corticosteroids

become quiescent upon using TAC immunosuppressant [2-4].

The drug works by attaching to the immunophilin FK506-binding protein (FKBP12), forming a complex that prevents nuclear factor of activated T cells (NFAT) from being dephosphorylated by calcineurin, thereby preventing the transcription of interleukin-2 (IL-2) and T cell-mediated actions.[3,5]. Moreover, TAC suppresses B cell-mediated immunity, significantly decreasing inflammatory cells. Therefore, it is a good immunomodulator, suppressing the inflammation associated with ulcerative colitis, and oral diseases such as labial discoid lupus erythematosus, and oral lichen planus [6,7].

The documented multi-organs toxicities are the main clinical TAC-induced morbidity obstacle. TAC has adversely affected the pancreatic islets and kidneys, with even induction of post-implant diabetes mellitus [8]. Moreover, the TAC regimen has also altered bone metabolism and increased fracture risk [9]. Additionally, many studies have shown the effect of TAC on skin atrophy and collagen synthesis [6,10]. Peroral, TAC has induced gingival hyperplasia, though less than cyclosporine immunosuppressant in a case report [11]. Moreover, in vivo TAC administration has caused damage to the structure of the tongue mucosa and associated minor salivary tissue [2]. Additionally, TAC has induced mucosal pigmentation on topical application [12].

Oral administration of activated charcoal (AC) has been evident in treating the side effects of immunosuppressants and many drug-induced toxicoses [13,14]. Production of AC commences by heating bamboo or wood and proceeds by its conversion into powder with micro-porosities to increase its surface area, attaining absorbent properties to the charcoal [15]. With its potent anti-inflammatory and detoxifying actions, AC has treated many intoxications via the chelation of these medicaments, phytotoxins, and toxic chemicals onto its surface, stopping their intestinal absorption [16]. Therefore, oral intake of AC effectively suppresses post-radiation systemic alterations and reduces the mucosal aberrations in the spleen and small intestine [17]. Further, charcoal has many dermatological uses for its antiaging and smoothening effects [15].

In the present work, we tested the efficiency of AC as a protective measurement taken concurrently with TAC to counteract its side effects on lingual mucosa. We tested our hypothesis in vivo by examining the influence of TAC on rat lingual mucosae dorsally and ventrally, besides the lingual minor salivary glands, and to detect the possible healing effect of the concomitant-administered AC. Our morphometric and immunohistochemical results revealed the antidegenerative properties of AC protecting the lingual structure against TAC-induced atrophy.

MATERIALS AND METHODS

2.1 Animals and sample size estimation

The current experiment was carried out on 30 male adult Wistar albino rats aged 12 weeks and weighed 220-240 grams. Rats having any disease or wounds or that were already enrolled in researches or altered genetically were not included [18]. Animal acclimatization was for two weeks in the housing facilities of the Faculty of Medicine, Alexandria University. Rats were maintained under 12:12 h day/night cycles in well-ventilated wire mesh bottom cages at 24 ± 2 °C with controlled humidity and

noise. They received water and diet throughout the experimental duration with monitoring of their normal behavior. The study commenced after being approved by the Scientific Research Ethics Committee, Faculty of Dentistry, Alexandria University (0681-0512023). All procedures followed the guidelines of the Alexandria University Ethics Committee for Animal Experimentation and are in adherence to the ARRIVE guidelines [19].

Assuming an effect size of 65 ± 4.3 according to Masson's trichrome stain analysis results of the control and immunosuppressant groups [2], the minimal total sample size was hypothesized to be 30 rats (10 per group) to investigate the efficacy of AC against the degenerative changes in the lingual mucosa of Wistar albino rats treated by TAC immunosuppressant. The study sample was calculated by Power Analysis and Sample Size Calculator (PASS 2020, GPower version 3.1.9.2), taking an alpha error of 5% and power of 80% using an independent t-test [20].

2.2 Study design and randomization

Allocation of the animals to three equal cohorts (n = 10 each) was random, using a random number generator software (Prism G. version 5.04, CA, USA) [18].

Rats in the control group received daily subcutaneous saline injections, whereas those in the TAC group received daily subcutaneous injections of 1.5 mg/Kg saline-dissolved TAC [8]. In the TAC+AC group, besides the daily regimen of subcutaneous TAC injections, rats received concomitant oral administrations of AC (0.5 g/Kg) by oral gavage [21]. The experiment lasted for three weeks, after which rats were euthanized by an intravenous overdose of barbiturates as 120 mg/Kg pentobarbital sodium (Nembutal, Akorn, Illinois, USA). Confirmation of animal death was cautiously assessed, with handling the remains of animal bodies by special authorities [22].

2.3 Histological evaluation

The tongues from the total 30 rats (n = 10 per group) were dissected sagittally into two halves, and the Weber glands were separated. 10% neutral buffered formalin-fixed specimens were alcohol-xylene processed for paraffin wax embedding. Then, 4-5 μ m sections were hematoxylin and eosin (H&E)-stained for histological evaluation. In addition, Masson trichrome was performed for the demonstration of collagen fibers [2]. The qualitative examination of the ventral and dorsal lingual mucosae with their associated minor salivary gland tissue was double blinded by 1st and 2nd authors, seeking signs of mucosal changes, glandular vacuolations, and cystic transformation. Captured photomicrographs were at $\times 100$ and $\times 400$ magnifications using a digital camera coupled to the microscope (Optika, B-290, SN 589279 series, Ponteranica, Italy).

2.4 Immunohistochemical analysis

Evaluating the melanocytic effect of TAC (n = 5 per group), rat tongue specimens were stained by mouse monoclonal to Melan A antibodies (M2-9E3; Abcam) following the universal peroxidase-labeled streptavidin-biotin technique. Briefly, 3-4 μ m paraffin sections were incubated with primary antibody and washed in phosphate-buffered saline (PBS). Then, a secondary antibody associated with Envision System was applied. After PBS wash, the chromogenic antigen-antibody reaction detection was through 3,3 diaminobenzidine application followed by hematoxylin-counterstaining [23].

2.5 Histomorphometric analysis

Histomorphometric analysis of the Masson trichrome sections assessed the mean collagen surface area (n = 10 per group). Furthermore, the immunomorphometric for Melan-A was in terms of mean area percent and optical density (n = 5 per group) [24]. The morphometric analyses were measured among groups by double-blinded investigators on \times 400-captured photomicrographs at standardized depths, using Image J software version 1.54d (1.53K, NIH, USA).

2.6 Statistical analysis

IBM SPSS software package version 20.0. (Armonk, NY: IBM Corp) was used for data analysis. Continuous data were tested for normality by the Shapiro-Wilk test. The three studied groups were compared using one-way ANOVA test, followed by a Post Hoc test (Tukey) for pairwise comparisons between every two groups. Data expression is through mean \pm standard deviation (SD) for normally distributed quantitative variables. Setting of the significant value was at 5%, with $p > 0.05$.

RESULTS

3.1 Activated charcoal restores the mucosal histological lingual structure altered by tacrolimus.

The dorsal lingual mucosal surface in the control group was covered by keratinized squamous epithelium with epithelial ridges projecting into the connective tissue, overlying the central muscular lingual core, formed of striated muscle fibers as bundles oriented in 3 different directions. The lingual epithelium displayed numerous thread-like filiform papillae and fewer mushroom-shaped fungiform papillae with taste buds on their superior border. Characteristically, the thin keratinized stratified squamous epithelium, investing the ventral lingual surface, was formed of 6-8 epithelial cell layers with shallow epithelial ridges. Dispersed clear non-keratinocytes cells were noted basally among the epithelial cell population of both surfaces (Fig. 1a).

TAC administration altered the dorsal lingual epithelial surface with atrophic changes encountered in the filiform papillae, represented by their flat appearance in focal spots. Interestingly, numerous noticeable non-keratinocytes were revealed basally, in addition to nuclear hyperchromatism throughout epithelial layers, with increased nuclear-cytoplasmic ratio and boosted granular content. Furthermore, the fungiform papillae showed areas of degenerated taste buds, and the ventral mucous membrane of the tongue displayed localized epithelial atrophy with loss of rete pegs and thinning keratinous layer (Fig. 1b).

Co-administration of AC with TAC regained the regular histological lingual structure. The dorsal epithelial lining in the TAC+AC group exhibited standard configured filiform and fungiform papillae, with a diminished prevalence of clear cells. The ventral surface of the tongue showed enhanced epithelial thickness and shallow epithelial ridges (Fig. 1c).

3.2 Reinforcement of the degenerated subepithelial TAC-treated collagen fibers by activated charcoal.

The underlying lamina propria dorsally and ventrally in the control group showed thick bundles of collagen fibers and associated spindle-shaped fibroblasts and blood capillaries (Fig. 2). Meanwhile, the disarranged collagen fibers within the lamina propria of the TAC-treated lingual mucosa showed pale Masson staining and areas of degeneration. Further, TAC administration elicited dilatation of congested blood vessels seen engorged with red blood cells (Fig. 2b). Chelating down the degenerative effect of TAC with AC, the lamina propria re-displayed densely packed bundles of collagenous fibers with no signs of degeneration, except in focal regions occasionally seen. Normal vascularity comparable to the control group was also noticed (Fig. 2c).

Morphometrically, as shown in Figure 3, the mean area percent, recording $5.34 \pm 0.89\%$ of Masson-positive collagenous fibers in the TAC group, is significantly lower than both the control and TAC+AC groups ($9.1 \pm 2.43\%$ of $p < 0.001$ and $9.18 \pm 2.4\%$ of $p < 0.001$, respectively). Moreover, the collagen fibers in the TAC+AC group reveal a similar mean area percent as the control group ($p = 0.997$).

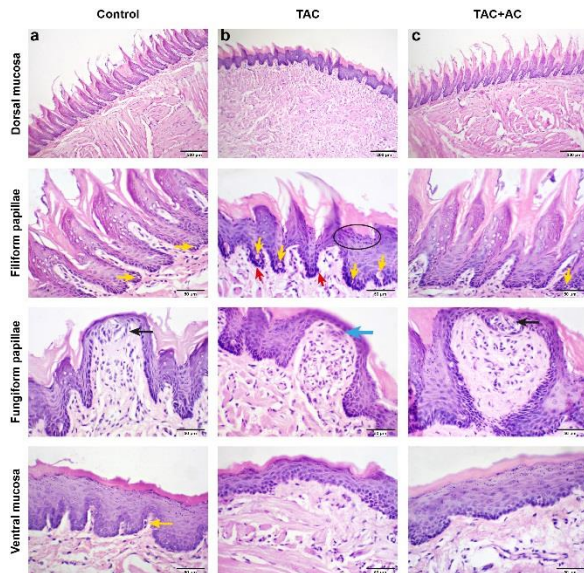


Figure 1: Representative H&E-stained photomicrographs of the rat lingual mucosae of the different groups: (a) The control group shows the dorsal surface of the tongue overlying the muscular core with numerous thread-like filiform papillae covered by a layer of keratinized squamous epithelium showing dispersed clear cells (yellow arrows) and epithelial ridges projecting into the connective tissue. The normal mushroom-shaped fungiform papillae show the taste buds on their superior surface (black arrow), and the ventral surface is invested by the thin keratinized squamous epithelium of 6-8 epithelial layers with shallow epithelial ridges and dispersed clear cells (yellow arrow). (b) TAC group shows the dorsal lingual epithelium with atrophic filiform papillae in focal spots and numerous basal non-keratinocytes (yellow arrows) in addition to hyperchromatic nuclei of epithelial cells basally (red arrows) and increased granular content (circle). Furthermore, the fungiform papillae reveal degenerated taste buds (black arrow), and the ventral lingual surface shows localized epithelial thinning, thin keratin, and loss of rete pegs. (c) TAC+AC group exhibits normal histological structure and appearance of the dorsal epithelial lining with less prevalent clear cells (yellow arrow) along the filiform papillae. The fungiform papillae restore their taste bud on the upper surface (black arrow), and the ventral surface preserves its epithelial thickness and keratinization with shallow epithelial ridges (Scale bar = 200 μm is $\times 100$, while scale bar = 50 μm is $\times 400$).

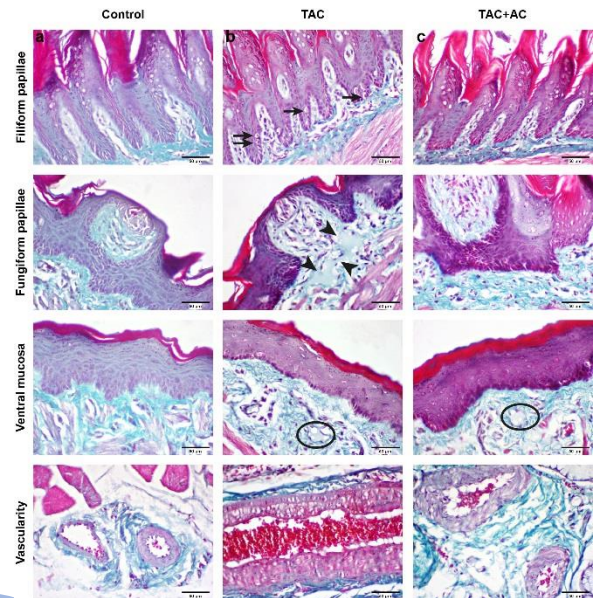


Figure 2: Representative Masson trichrome-stained photomicrographs of the lamina propria of the lingual mucosa in different groups: (a) The control group reveals thick bundles of collagen fibers underlying the filiform and fungiform papillae dorsally and ventrally, as well as normal blood capillaries within connective tissue. (b) TAC group shows scattered collagen fibers underlying filiform papillae, reporting numerous non-keratinocytes (black arrows). The lamina propria of fungiform papillae displays areas of collagen degeneration (arrowheads), irregular pale staining fibers on the ventral side, noting the spot of degenerated collagen (circle). The associated blood vessels are dilated and engorged with red blood cells. (c) TAC+AC group displays densely packed bundles of collagenous fibers in lamina propria of the filiform and fungiform papillae along with the ventral surface that reveals a focal region of degeneration (circle), yet with normal vascularity (scale bar = 50 μm is $\times 400$).

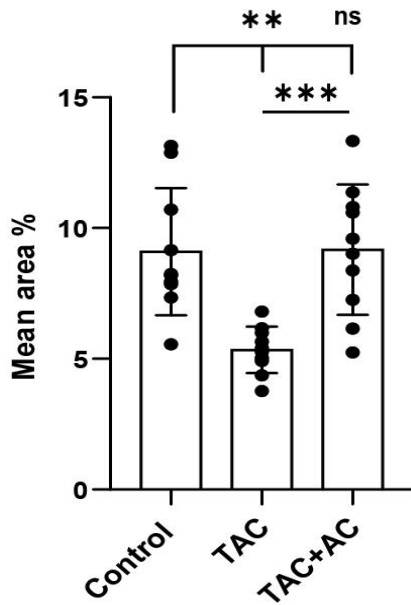


Figure 3: Morphometric analysis of the fibrotic index between different groups: The scatter dot plot shows the significant decrease in the mean area of Masson trichrome-positive stained collagen fibers in the TAC group, which returns to normal percent indifferentially to the control in the TAC+AC group (** $p < 0.01$, *** $p < 0.001$, and ns is non-significant of $p > 0.05$).

3.3 Lingual minor salivary glands return formally upon charcoal co-administration.

Concerning mucous acini, the posterior-located acini of Weber minor salivary glands showed the standard tubular structure and foamy mucinous secretory granules separated by thin connective tissue septa and muscle fibers (Fig. 4a-b). However, TAC-treated distended mucous acini revealed very wide lumina and evident cystic transformation surrounded by intense extravasated red blood cells (Fig. 4c-d). In the TAC+AC group, the secretory mucous acini were of regular size, and cystic transformations were reduced to a great extent and interspersed by normal-sized blood vessels with no signs of congestion (Fig. 4e-f). In a more anterior position, serous acini with short ducts were located between the lingual muscle fibers, showing a rounded structure with round basal-located nuclei (Fig. 5a-b). In the TAC group, the serous acini displayed shrinkage, mild acinar and ductal cytoplasmic vacuolations, and distorted boundaries (Fig. 5c-d). Meanwhile, the serous acini showed a preserved typical structure without vacuolations upon concurrent local administration of AC with TAC (Fig. 4e-f).

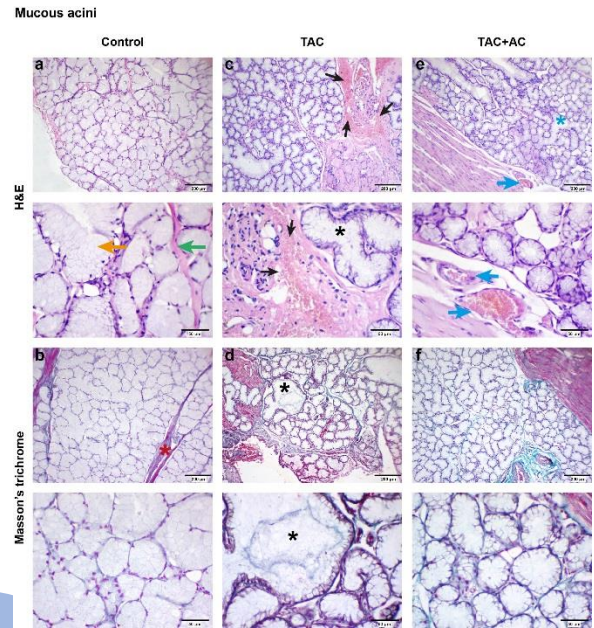


Figure 4: Evaluation of the effect of different treatment panels on the mucous acini of Weber minor salivary glands: (a-b) The control group shows the standard tubular structure and foamy mucinous secretory granules (yellow arrow) separated by thin connective tissue septa (green arrow) and muscle fibers (red asterisk). (c-d) TAC group reveals distended mucous acini with very wide lumina and evident cystic transformation (black asterisks) surrounded by intense extravasated red blood cells (black arrows). (e-f) The secretory portions in the TAC+AC group restore the regular size with a reduction in the cystic transformation to a great extent (blue asterisk), interspersed by normal-sized blood vessels with no signs of congestion (blue arrows). (a, c, and e) are H&E-stained, (b, d, and f) are Masson trichrome-stained, (Scale bar = 200 μm is $\times 100$, while scale bar = 50 μm is $\times 400$).

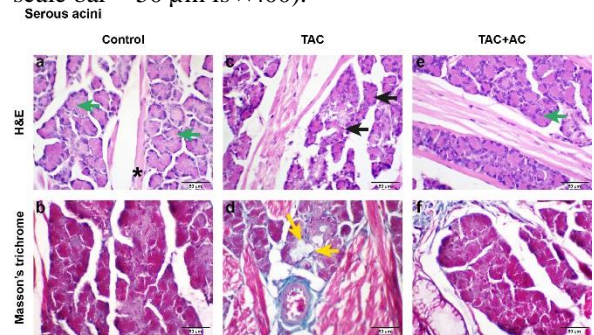


Figure 5: Histological examination of the lingual serous acini in different groups: (a-b) The control group shows round structures with basal nuclei (green arrows) separated by the tongue muscle fibers (black asterisk). (c-d) TAC group shows shrunken serous acini (black arrows) with mild acinar and ductal cytoplasmic vacuolations (yellow arrows). (e-f)

TAC+AC group preserves the acinar structure without vacuolations (green arrow). (a, c, and e) are H&E-stained, (b, d, and f) are Masson trichrome-stained, (Scale bar = 50 μ m is \times 400).

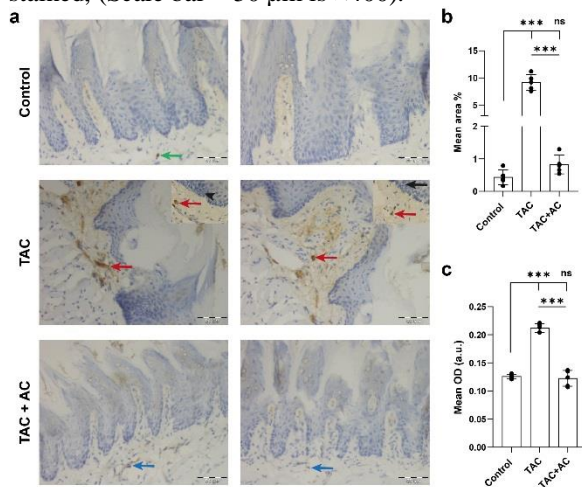


Figure 6: Melanocytes immune-morphometric analysis among different groups. (a) Melan A immunohistochemical-stained photomicrographs (\times 400) reveal the few scattered positive stained melanophages within the connective tissue of the control group (green arrow). The melanophages increase upon TAC treatment (red arrows) with detected melanocytes along the basal cells (arrowhead in inset \times 1000). The black arrow points out the mitotic activity observed in the TAC group. The number of melanophages (blue arrows) returns almost to normal levels in the TAC+AC group. (b-c) Scatter dot plots of the mean area percent (MA%) and mean optical density (OD) of Melan A, respectively, where the immuno-positivity increases significantly (***) in both terms with TAC. Meanwhile, counteracting the TAC with AC yields the MA% and OD indifferent (ns; $p > 0.05$) to the control.

3.4 The reduced melanocytic activity of activated charcoal

Immunohistochemically, normal lingual mucosa revealed almost negative Melan-A-stained basal cells with no detectable melanophages in the lamina propria. Upon TAC treatment, the immunosuppressive agent triggered the melanin production, both basally and sub-basally, with noticeable detected melanocytes and melanophages, respectively. With AC protective mechanisms, few scattered Melan-A positive-stained melanophages with almost undetectable melanocytes along the basal cell layer (Fig. 6a). A reflected morphometric picture in Figure 6b-c, where Melan-A positivity reduced significantly almost to the control level in the TAC+AC group, recording mean area percent of $0.82 \pm 0.2\%$ and optical density of 0.12 ± 0.01 a.u. ($p >$

0.05), after their respective substantial raises with single TAC treatment to $9.1 \pm 1.4\%$ and 0.21 ± 0.00 a.u. ($p < 0.0001$).

DISCUSSION

The innate immune system's function is to defend the body against various insults by activating macrophages, T lymphocytes, and a variety of other inflammatory cytokines. [25]. Suppression of the immune system is mandatory following solid organ transplantation to control acute and chronic allograft rejection [26].

Tacrolimus is one of the potent anti-T-lymphocyte immunomodulators produced by the fungus *Streptomyces tsukubaensis*. TAC is one of the most currently used immunosuppressants in organ transplantation and autoimmune disorders [6,27]. However, its reported organ toxicity is one of the TAC-associated main adverse effects. Therefore, the current research tested the efficacy of AC in reducing the damage caused by the systemic administration of TAC in the lingual mucosa and the associated minor salivary tissue.

The animal model in the current study was Wistar rats due to their numerous similarities in tongue structure shared with humans. The dorsal keratinized surface reveals the characteristic lingual papillae: filiform, fungiform, and occasionally circumvallate. Unlike humans, the rat ventral lingual mucosa consists of keratinized stratified squamous epithelium [28,29].

Histological analysis of the present study revealed that TAC promoted atrophic changes in focal areas along both tongue surfaces dorsal as well as ventral, besides other degenerative changes in the epithelium, such as the degeneration of taste buds of the fungiform papillae. Also, serous acini showed intracytoplasmic vacuolation, and the mucous acini showed cystic degeneration. In accordance, TAC has altered the parenchymal structures of rats' parotid and submandibular glands, including distortion of the acini, atypical mitosis, and hyperchromasia [30]. Rather than oral degenerative effects, other tissues have reported similar changes upon TAC administration, where the epithelium of testicular tubules revealed epithelial atrophy in addition to deeply stained nuclear chromatin and abundant vacuoles [31]. The adverse impact of TAC has expanded to the renal tissue, with massive vacuolization and fibrosis as signs of nephrotoxicity [32].

Our findings also demonstrated the degeneration of the collagen fibers that appeared less scattered and distorted in the TAC group. This observation agreed with the *in vivo* histological work on the impact of immunosuppressing agents on the tongue of rodents, which revealed that TAC provoked the deterioration of collagen fibers within the lingual lamina propria [2]. The

TAC-induced injury could result from the oxidative stress it produces in different tissues and organs [8].

The histomorphometric analysis of our study revealed that the surface area of the collagen fibers in TAC-treated rats was less than both the control and AC group, which might indicate the degenerative changes of TAC on the collagen fibers within the connective tissue of rat's tongue with the protective efficacy of AC on the collagen. In correlation to these findings, AC has maintained the intact connective tissue fibers and prevented kidney fibrosis, as reported in a study case, where AC could be beneficial in treating the early stage of kidney disease through its anti-inflammatory action [33].

Besides, the epithelial-mucosal layers in the TAC+AC group showed markedly less atrophy and degeneration. Activated carbon, in accordance, has prevented the atrophic and degenerative changes induced in the intestinal mucosa by acute radiation [17]. Moreover, charcoal supplementation has preserved the structure of minor salivary gland tissue with enhancing action. The citric acid and sodium bicarbonate in the carbonic acid tablets, which were studied on the submandibular and sublingual glands, were found to stimulate their secretory function, notably from the submandibular gland. [34].

In the present study, there was an increase in the number of non-keratinocytes, with an increase in the immunoreaction to Melan-A in the TAC-treated group. Per this finding, TAC treatment has resulted in mucosal staining in a case report attributed to melanin incontinence as well as destruction in keratinocytes cells with mild inflammation [12]. In this work, the immunoreaction to Melan-A decreased in the AC-treated group, suggesting that melanocytes decreased after charcoal treatment.

In conclusion, the present study revealed that the charcoal-treated group showed enhancement in both epithelial and connective tissue architecture of the tongue, mucous and serous acini, which might be due to the protective action of charcoal in the treatment of toxicosis. Activated charcoal adsorbs ingested toxins within the gastrointestinal tract hindering the systemic absorption of that toxin [13,16]. Moreover, our observations suggest that the degenerative effects of tacrolimus were temporary. Co-therapy of charcoal with immunosuppressant drugs could improve their adverse actions. However, our results are limited to male rats, with further studies needed to involve female rats before studying the protective potential of AC in the clinical setting.

Declarations

Acknowledgments

The authors are grateful to the Center of Excellence for Research in Regenerative Medicine and Applications (CERRMA), Faculty of Medicine,

Alexandria University (STDF-Funded) for the assistance provided by the staff in the microscopic unit. Also, we extend our thanks to the staff in the Animal House, Faculty of Medicine, Alexandria University for their professional academic handling of the rats.

Author contributions

Conceptualization, methodology, validation, data curation, research conduction, resources, original writing draught preparation, visualisation, and writing-reviewing and editing were the responsibilities of Hagar S. Abdel Fattah. Formal analysis, research, resources, software, writing-review, and editing by Marwa M. Essawy. Conceptualization, methodology, validation, data curation, research, resources, writing-first draught preparation, and visualisation were all done by Amira S. Eissa.

Funding

The authors received no specific funding for the study.

Availability of data and materials

The presented publication includes all the materials and datasets that were used in the current investigation.

Ethical approval

The Scientific Research Ethics Committee, Faculty of Dentistry, Alexandria University, Egypt has approved this animal study (IORG 0008839). The current study's manuscript strictly adheres to the ARRIVE guidelines.

Competing interests

The authors declare no competing interests.

Conflict of interest

The authors declare that they have no conflict of interest.

REFERENCES

1. Banas B, Krämer BK, Krüger B, Kamar N, Undre N. Long-Term Kidney Transplant Outcomes: Role of Prolonged-Release Tacrolimus. *Transplant Proc* 2020; 52: 102-10. <https://doi.org/https://doi.org/10.1016/j.transproceed.2019.11.003>.
2. Mahmoud LDE-d, Ghali LS, Selim M. Histological study on the effect of the immunosuppressive drugs on the mucous membrane and salivary glands of the treated rats tongues. *Dental Science Updates* 2021; 2: 1-7.
3. Dheer D, Jyoti, Gupta PN, Shankar R. Tacrolimus: An updated review on delivering strategies for multifarious diseases. *Eur J Pharm Sci* 2018; 114: 217-27. <https://doi.org/https://doi.org/10.1016/j.ejps.2017.12.017>.

4. Ong SC, Gaston RS. Thirty Years of Tacrolimus in Clinical Practice. *Transplantation* 2021; 105: 484-95. <https://doi.org/10.1097/tp.0000000000003350>.
5. Zidan M, Pabst R. Histological characterization of the lingual tonsils of the one-humped camel (*Camelus dromedarius*). *Cell Tissue Res* 2020; 380: 107-13. <https://doi.org/10.1007/s00441-019-03135-2>.
6. Umar BU, Rahman S, Dutta S, Islam T, Nusrat N, Chowdhury K et al. Management of Atopic Dermatitis: The Role of Tacrolimus. *Cureus* 2022; 14.
7. Yu Y, Zhong J, Peng L, Wang B, Li S, Huang H et al. Tacrolimus downregulates inflammation by regulating pro-/anti-inflammatory responses in LPS-induced keratitis. *Mol Med Rep* 2017; 16: 5855-62. <https://doi.org/10.3892/mmr.2017.7353>.
8. Ko EJ, Shin YJ, Cui S, Lim SW, Chung Byung H, Yang CW. Effect of dual inhibition of DPP4 and SGLT2 on tacrolimus-induced diabetes mellitus and nephrotoxicity in a rat model. *American Journal of Transplantation* 2022; 22: 1537-49. <https://doi.org/https://doi.org/10.1111/ajt.17035>.
9. Kanda J, Izumo N, Furukawa M, Shimakura T, Yamamoto N, E. Takahashi H et al. Effects of the calcineurin inhibitors cyclosporine and tacrolimus on bone metabolism in rats. *Biomedical Research* 2018; 39: 131-9. <https://doi.org/10.2220/biomedres.39.131>.
10. Reitano S, Rissanen J, Remitz A, Granlund H, Erkkö P, Autio P et al. Tacrolimus Ointment does not Affect Collagen Synthesis: Results of a Single-Center Randomized Trial. *J Invest Dermatol* 1998; 111: 396-8. <https://doi.org/https://doi.org/10.1046/j.1523-1747.1998.00323.x>.
11. Nivethitha K, Ramesh A, Talwar A, Shenoy N. Rare phenomena of tacrolimus-induced gingival hyperplasia. *J Oral Maxillofac Pathol* 2020; 24: 403. https://doi.org/10.4103/jomfp.JOMFP_50_20.
12. Fricain J, Sibaud V, Campana F, Lepreux S, Taieb A. Mucosal pigmentation after oral lichen planus treatment with topical tacrolimus. *Dermatology* 2005; 210: 229-32.
13. Qualls HJ, Holbrook TC, Gilliam LL, Njaa BL, Panciera RJ, Pope CN et al. Evaluation of Efficacy of Mineral Oil, Charcoal, and Smectite in a Rat Model of Equine Cantharidin Toxicosis. *J Vet Intern Med* 2013; 27: 1179-84. <https://doi.org/https://doi.org/10.1111/jvim.12164>.
14. Yeh C-N, Hsieh C-H, Chao-Ming H, Long-Bin BJ. Acute overdoses of tacrolimus (FK 506). *Digestive diseases and sciences* 1999; 44: 1650.
15. Sanchez N, Fayne R, Burroway B. Charcoal: An ancient material with a new face. *Clin Dermatol* 2020; 38: 262-4. <https://doi.org/https://doi.org/10.1016/j.clinidmatol.2019.07.025>.
16. Zellner T, Prasa D, Färber E, Hoffmann-Walbeck P, Genser D, Eyer F. The Use of Activated Charcoal to Treat Intoxications. *Dtsch Arztebl Int* 2019; 116: 311-7. <https://doi.org/10.3238/arztebl.2019.0311>.
17. Snezhkova E, Rodionova N, Bilko D, Silvestre-Albero J, Sydorenko A, Yurchenko O et al. Orally administered activated charcoal as a medical countermeasure for acute radiation syndrome in rats. *Applied Sciences* 2021; 11: 3174.
18. Johnson PD, Besselsen DG. Practical aspects of experimental design in animal research. *ILAR journal* 2002; 43: 202-6.
19. Percie du Sert N, Hurst V, Ahluwalia A, Alam S, Avey MT, Baker M et al. The ARRIVE guidelines 2.0: Updated guidelines for reporting animal research. *J Cereb Blood Flow Metab* 2020; 40: 1769-77.
20. Muralidharan K. *Sample Size Determination. Six Sigma for Organizational Excellence*: Springer; 2015. p. 81-97.
21. Hanan AA, Riham MR. Effect of lead toxicity on cytogenicity, biochemical constituents and tissue residue with protective role of activated charcoal and casein in male rats. *Aust J Basic Appl Sci* 2012; 7: 497-509.
22. Council NR. *Guide for the care and use of laboratory animals*. 2010.
23. Essawy MM, El-Sheikh SM, Raslan HS, Ramadan HS, Kang B, Talaat IM et al. Function of gold nanoparticles in oral cancer beyond drug delivery: Implications in cell apoptosis. *Oral Dis* 2021; 27: 251-65. <https://doi.org/10.1111/odi.13551>.
24. El-Habashy SE, El-Kamel AH, Essawy MM, Abdelfattah EA, Eltaher HM. 3D printed bioinspired scaffolds integrating doxycycline nanoparticles: Customizable implants for in vivo osteoregeneration. *Int J Pharm* 2021; 607: 121002. <https://doi.org/10.1016/j.ijpharm.2021.121002>.
25. Diamond MS, Kanneganti T-D. Innate immunity: the first line of defense against SARS-CoV-2. *Nature Immunology* 2022; 23: 165-76. <https://doi.org/10.1038/s41590-021-01091-0>.
26. Vaillant AAJ, Mohseni M. *Chronic Transplantation Rejection. StatPearls [Internet]*: StatPearls Publishing; 2021.
27. Assmann T, Homey B, Ruzicka T. Applications of tacrolimus for the treatment of skin disorders. *Immunopharmacology* 2000; 47: 203-13.

28. Abayomi TA, Ofusori DA, Ayoka OA, Odukoya SA, Omotoso EO, Amegor FO et al. A Comparative Histological Study of the Tongue of Rat (*Rattus Norvegicus*), Bat (*Eidolon Helvum*) and Pangolin (*Manis Tricuspis*). *International Journal of Morphology* 2009; 27.
29. Thirion-Delalande C, Gervais F, Fisch C, Cuiné J, Baron-Bodo V, Moingeon P et al. Comparative analysis of the oral mucosae from rodents and non-rodents: Application to the nonclinical evaluation of sublingual immunotherapy products. *PLoS One* 2017; 12: e0183398. <https://doi.org/10.1371/journal.pone.0183398>.
30. Spolidorio LC, Herrera BS, Coimbra LS, de Andrade CR, Spolidorio DMP, Rossa Junior C et al. The long-term administration of calcineurin inhibitors decreases antioxidant enzyme activity in the rat parotid and submandibular salivary glands. *Life Sci* 2015; 134: 1-8. <https://doi.org/https://doi.org/10.1016/j.lfs.2015.04.022>.
31. Caneguim BH, Cerri PS, Spolidório LC, Miraglia SM, Sasso-Cerri E. Structural alterations in the seminiferous tubules of rats treated with immunosuppressor tacrolimus. *Reproductive Biology and Endocrinology* 2009; 7: 19. <https://doi.org/10.1186/1477-7827-7-19>.
32. Fu R, Tajima S, Shigematsu T, Zhang M, Tsuchimoto A, Egashira N et al. Establishment of an experimental rat model of tacrolimus-induced kidney injury accompanied by interstitial fibrosis. *Toxicol Lett* 2021; 341: 43-50. <https://doi.org/https://doi.org/10.1016/j.toxlet.2021.01.020>.
33. El-Kafoury B, Saleh N, Saad D, Shawky M, Mahrose E. Role of activated charcoal in limiting the progression of chronic kidney disease in experimental albino rats. *QJM: An International Journal of Medicine* 2018; 111: hcy200. 190.
34. Yamamoto K, Yamamoto S, Yanagisawa Y. Carbonic acid tablets promote submandibular-sublingual salivary secretion in humans. *J Funct Foods* 2020; 74: 104173. <https://doi.org/https://doi.org/10.1016/j.jff.2020.104173>.